Available online at www.sciencedirect.com
ScienceDirect
Journal of the European Ceramic Society 28 (2008) 85–90
www.elsevier.com/locate/jeurceramsoc

# Effect of bismuth addition on the electrical conductivity of gadolinium-doped ceria ceramics

Yen-Pei Fu *, Chien-Wei Tseng, Po-Chin Peng

*Department of Materials Science and Engineering, National Dong-Hwa University, Shou-Feng, Hualien 974, Taiwan*

Received 1 December 2006; received in revised form 23 April 2007; accepted 5 May 2007
Available online 20 July 2007

**Abstract**

The structure, thermal expansion and electrical conductivity of $Ce_{0.8}(Gd_{1-x}Bi_x)_{0.2}O_{1.9}$ ($x = 0.1$–$0.5$), prepared by coprecipitation were investigated. $Ce_{0.8}(Gd_{1-x}Bi_x)_{0.2}O_{1.9}$ ceramics was sintered in the range of 1350–1450 °C for 6 h; the bulk density of $Ce_{0.8}(Gd_{1-x}Bi_x)_{0.2}O_{1.9}$ ceramics was over 95% of the theoretical density; the maximum electrical conductivity, $\sigma_{800\,^\circ C} = 0.078$ S/cm with minimum activation energy, $E_a = 0.638$ eV was found for the $Ce_{0.8}(Gd_{0.5}Bi_{0.5})_{0.2}O_{1.90}$ ceramic. The gadolinium-doped ceria ceramics preparation by coprecipitation can reduce the sintering temperature by addition of bismuth. The thermal expansion coefficient of $Ce_{0.8}(Gd_{1-x}Bi_x)_{0.2}O_{1.9}$ covers the range of 20.132–20.478 ppm/°C. The ceramic has a fracture toughness in the range of 1.28–2.60 MPa $m^{1/2}$ for dense $Ce_{0.8}(Gd_{1-x}Bi_x)_{0.2}O_{1.9}$ ceramics. The value of fracture toughness increased with Bi content. It indicated that the mechanical properties of gadolinium-doped ceria ceramics could be improved by addition of bismuth.


*Keywords:* $CeO_2$; Mechanical properties; Solid oxide fuel cell

## 1. Introduction

A solid oxide fuel cell (SOFC) is a highly efficient power-generation system for future application. A typical high temperature SOFC uses 8 mol% yttria-stabilized zirconia (YSZ) as an electrolyte, which needs to operate at high temperatures of 800–1000 °C, where the ionic conductivity reaches the required high level. However, such high temperatures can to reaction between the components, thermal degradation or thermal expansion mismatch.[1] In order to reduce the operation temperature from 1000 to 800 °C or even lower, doped ceria has been considered as a promising solid electrolyte for moderate temperature solid oxide fuel cells.[2] The conductivity maximum in zirconia has been correlated with the minimum dopant level necessary to stabilize the high temperature face-centered cubic (fcc) phase. In contrast to pure zirconia, $CeO_{2-\delta}$, has the fluorite structure and oxygen vacancies ($V_o^{\bullet\bullet}$) as the predominant ionic defect.[3–5] Pure $CeO_2$ is a poor oxide ion conductor. However, the ion conductivity can be significantly improved by the substitution of gadolinium, compensated by oxygen vacancies,

$$Gd_2O_3 \xrightarrow{CeO_2} 2Gd'_{ce} + 3O^x_o + V_o^{\bullet\bullet}$$

It is well known that ceria-based ceramics are difficult to densify below 1500 °C. For cost effectiveness, lowering sintering temperature for solid electrolyte is desirable since the co-firing with the anode and cathode materials is possible. Ceria-based ceramics, however, have a sintering temperature, which varies from 1500 to 1700 °C, depending on the dopant, the starting powders and sintering method. This can lead to considerable grain coarsening and therefore poor mechanical properties.[6] In order to overcome the above-mentioned problem, bismuth can be added to reduce sintering temperature and grain growth. Chemical precipitation is a simple and feasible technique for synthesizing ultra fine ceramic powders with high sinterability. In the current research, we present the results of a systematic study of the structure, thermal expansion, mechanical and electrical properties of $Ce_{0.8}(Gd_{1-x}Bi_x)_{0.2}O_{1.9}$ prepared by coprecipitation process.

* Corresponding author. Tel.: +886 3 863 4209; fax: +886 3 863 4200.
*E-mail address:* d887503@alumni.nthu.edu.tw (Y.-P. Fu).

0955-2219/$ – see front matter © 2007 Published by Elsevier Ltd.
doi:10.1016/j.jeurceramsoc.2007.05.002

Table 1
Crystallite size of $Ce_{0.8}(Gd_{1-x}Bi_x)_{0.2}O_{1.9}$ powders prepared by coprecipitation process

| Composition | Crystallite size[a] (nm) |
|---|---|
| $X=0.1$ | 11.7 |
| $X=0.2$ | 14.9 |
| $X=0.3$ | 12.3 |
| $X=0.4$ | 12.4 |
| $X=0.5$ | 13.1 |

[a] Crystallite size measured from XRD line broadening.

## 2. Experimental procedures

### 2.1. Sample synthesis

Solid solution $Ce_{0.8}(Gd_{1-x}Bi_x)_{0.2}O_{1.9}$ ($x=0.1$–$0.5$) were synthesized by a coprecipitation method in this study. Stoichiometric amounts of cerium nitrate hexahydrate ($Ce(NO_3)_3{\cdot}6H_2O$), gadolinium nitrate hexahydrate ($Gd(NO_3)_3{\cdot}6H_2O$) and bismuth nitrate hexahydrate ($Bi(NO_3)_3{\cdot}6H_2O$) were dissolved in distilled water. Then the ammonia ($NH_4OH$) solution was added to nitrate solution, precipitates were form until pH 10. The resulting precipitate was vacuum-filtered, washed three times with water and ethanol, respectively, and dried at 90 °C in an oven. The coprecipitation hydrate powder decomposed to a polycrystalline oxide by heating to 600 °C for 2 h. The oxidation of $Ce^{3+}$ to $Ce^{4+}$ occurred during this stage. The powder sample were palletized and sintered at 1350–1450 °C for 6 h with a programmed heating and cooling rate of 5 °C/min. The sintered samples were over 95% of theoretical density in all specimens.

### 2.2. Characterization measurements

A computer-interface X-ray powder diffractometer (XRD, Rigaku D/Max-II, Japan) with Cu Kα radiation ($\lambda=0.15418$ nm) was used to identify the crystalline phase and determine mean crystalline size ($D_{XRD}$). $D_{XRD}$ was calculated according to Scherer equation: $D_{XRD}=0.9\lambda/B\cos\theta$, where λ is the wavelength of the radiation, $\theta$ is the diffraction angle and $B$ is the corrected half-width of the diffraction peak, given by $B^2=B_m^2-B_s^2$, where $B_m$ is the measured half-width of the diffraction peak and $B_s$ is the half-width of a standard $CeO_2$ with a crystal size greater than 100 nm. The reflection from (1 1 1) plane, occurring at 28.60 $2\Theta$, was used to calculate the crystallite size. The particle size determined from the broadening curve is about 11.7–14.9 nm in $Ce_{0.8}(Gd_{1-x}Bi_x)_{0.2}O_{1.9}$ samples. When using the Scherer equation, we assume that the particle size effects are only source of peak broadening; however, if compositional non-uniformity occurs in the particles, the particle size will be underestimated.

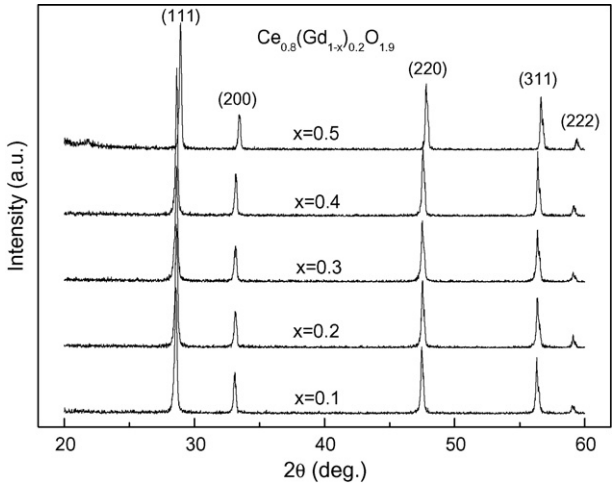


Fig. 1. XRD patterns of $Ce_{0.8}(Gd_{1-x}Bi_x)_{0.2}O_{1.9}$ ceramics.

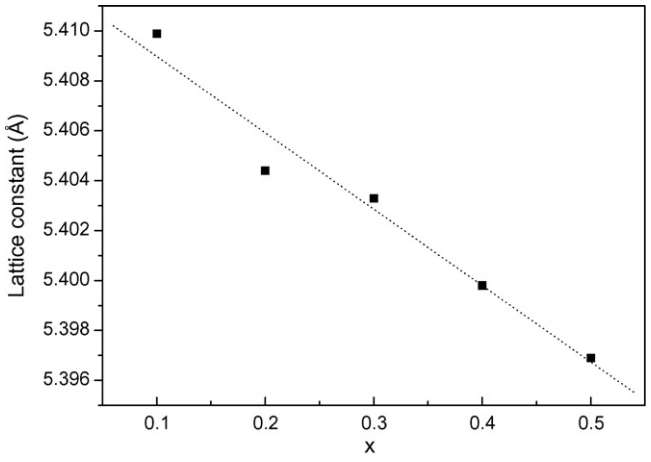


Fig. 2. Lattice constant of $Ce_{0.8}(Gd_{1-x}Bi_x)_{0.2}O_{1.9}$ ceramics as a function of $x$.

The morphological features of $Ce_{0.8}(Gd_{1-x}Bi_x)_{0.2}O_{1.9}$ ceramics were observed using a scanning electron microscope (SEM, Jeol JSM-6500F Japan). After sintering, the $Ce_{0.8}(Gd_{1-x}Bi_x)_{0.2}O_{1.9}$ samples were polished with diamond paste to 1 μm finish. They were then subjected to thermal etching by heating at 100 °C below sintering temperature for 1 h. For sintered specimens, the electrical conductivity was measured by two-point DC method on a sintered $Ce_{0.8}(Gd_{1-x}Bi_x)_{0.2}O_{1.9}$ pellet. The electrical conductivity measurements were made

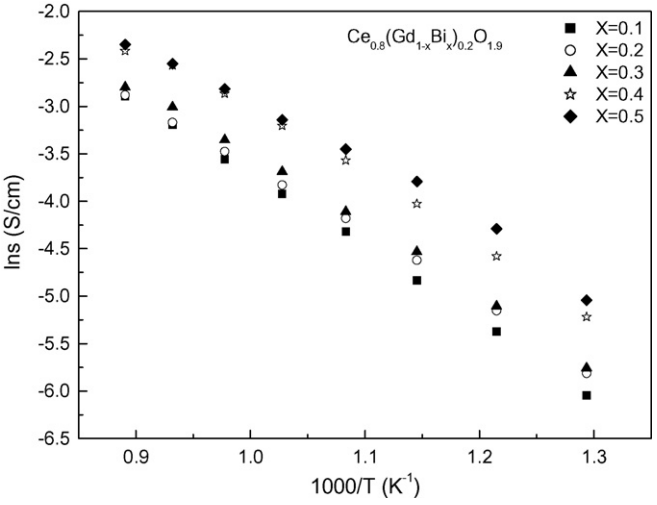


Fig. 3. Arrhenius plots for electrical conductivity of $Ce_{0.8}(Gd_{1-x}Bi_x)_{0.2}O_{1.9}$ ceramics.

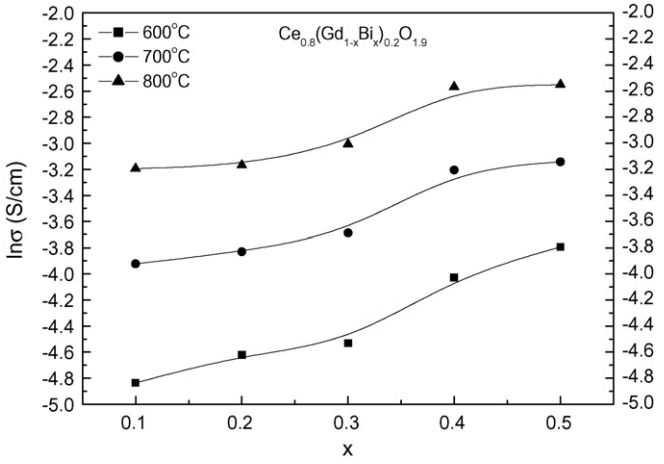


Fig. 4. Bi amount dependence of the electrical conductivity of $Ce_{0.8}(Gd_{1-x}Bi_x)_{0.2}O_{1.9}$ ceramics at different temperatures.

at various temperatures in the range of 500–800 °C in air. Arrhenius plots (plots of log$\sigma$ versus $10^3/T$) were constructed and activation energies for conduction were computed. The densities of sintered ceramics were measured by the Archimendean method. The thermal expansion coefficients of sintered $Ce_{0.8}(Gd_{1-x}Bi_x)_{0.2}O_{1.9}$ pellets were measured by dilatometer (DIL, Netzsch DIL 402 PC, Germany) using a constant heating rate of 10 °C/min in the temperature range of 25–850 °C.

Vickers hardness was measured using a microhardness tester (Akashi MVK-H110, Japan) with the load 1000 g, and held for 10 s. At least 10 indentations were used for obtained mean and standard deviation value of hardness and fracture toughness. All specimens were polished with a series of emery paper of 800, 1000, 1200 and 1500 grit. Contamination on the surface was ultrasonically cleaned with ethanol. The Vickers indenter hardness was determined by the average value of both diagonals with a Vickers indenter apex of 136° and calculated with follow equation: $H_V = 1.8544\,P/d^2$ where $P$ is the load and $d$ is the mean value of both diagonals.

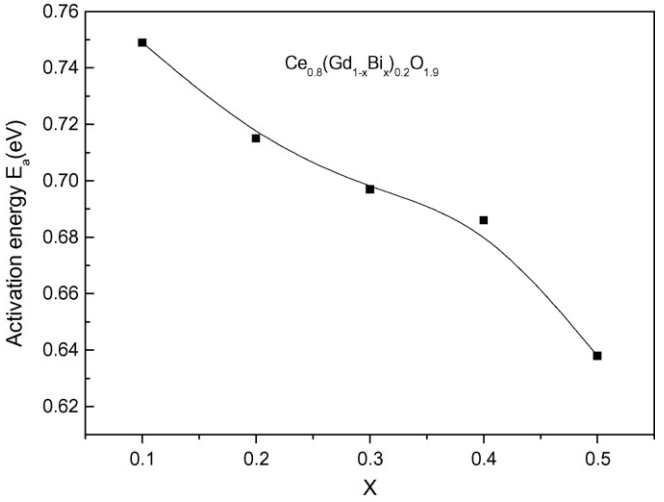


Fig. 5. Variation of the activation energy, $E_a$ as a function of Bi amount in $Ce_{0.8}(Gd_{1-x}Bi_x)_{0.2}O_{1.9}$ ceramics in the temperature range of 500–850 °C.

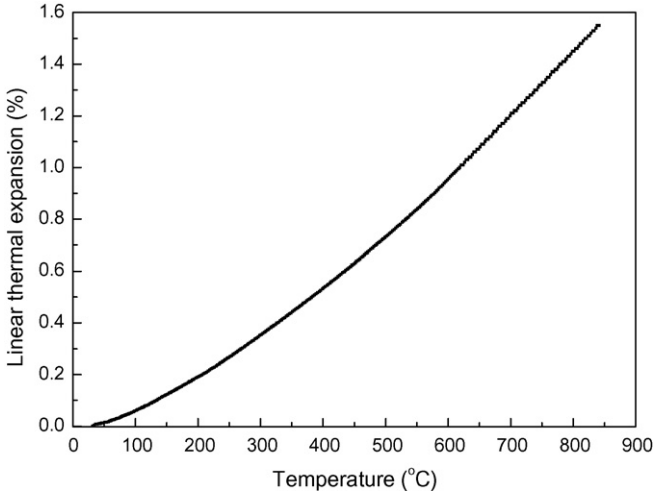


Fig. 6. Linear thermal expansion of $Ce_{0.8}(Gd_{0.9}Bi_{0.1})_{0.2}O_{1.9}$ ceramic as function of temperature in the range of 25–850 °C.

## 3. Results and discussion

The X-ray diffraction patterns of the $Ce_{0.8}(Gd_{1-x}Bi_x)_{0.2}O_{1.9}$ powders, which after calcined for 600 °C, were identified by the diffractometer. It is found that $Ce_{0.8}(Gd_{1-x}Bi_x)_{0.2}O_{1.9}$ powders contain only the cubic fluorite structure with space group Fm3m (JCPDS powder diffraction file no. 34-0384). Moreover, the XRD patterns peaks are quite broad and indicate the fine particle of the product. Table 1 summarizes the data of crystallite size of the $Ce_{0.8}(Gd_{1-x}Bi_x)_{0.2}O_{1.9}$ powder. The crystallite size calculated from peak broad ranges from 11.7 to 14.9 nm. The particle size calculated from specific surface area of the powders ranges from 18 to 50 nm and does not depend on the doping amount of bismuth. Fig. 1 displays the XRD patterns of $Ce_{0.8}(Gd_{1-x}Bi_x)_{0.2}O_{1.9}$ ceramics prepared by coprecipitation process with the fluorite structure in the Bi substitution in range of $x = 0.1$–0.5. No secondary phases are found in all specimens. It indicates a very large dopant concentration range for $Ce_{0.8}(Gd_{1-x}Bi_x)_{0.2}O_{1.9}$ ceramics ($x = 0.1$–0.5). The intro-

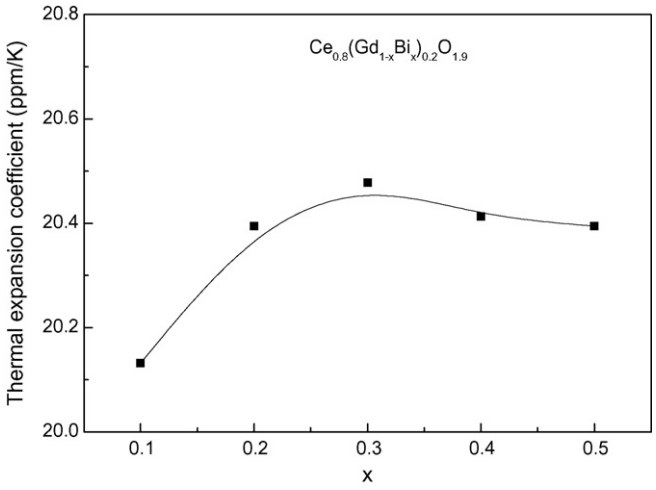


Fig. 7. Thermal expansion coefficient of $Ce_{0.8}(Gd_{1-x}Bi_x)_{0.2}O_{1.9}$ ceramics as a function of $x$.

Table 2
Relative density, electrical conductivity and activation energy of $Ce_{0.8}(Gd_{1-x}Bi_x)_{0.2}O_{1.9}$ ceramics

| Composition | Conductivity (S/cm) | | | Activation energy $E_a$ (eV) | Pre-exponential $\sigma_o$ (S, °C/cm) |
|---|---|---|---|---|---|
| | 600 °C | 700 °C | 800 °C | | |
| $X=0.1$ | $7.94\times10^{-3}$ | $1.98\times10^{-2}$ | $4.09\times10^{-2}$ | 0.749 | $1.45\times10^{5}$ |
| $X=0.2$ | $9.84\times10^{-3}$ | $2.17\times10^{-2}$ | $4.20\times10^{-2}$ | 0.715 | $1.18\times10^{5}$ |
| $X=0.3$ | $1.08\times10^{-2}$ | $2.50\times10^{-2}$ | $6.10\times10^{-2}$ | 0.697 | $8.64\times10^{4}$ |
| $X=0.4$ | $1.78\times10^{-2}$ | $4.05\times10^{-2}$ | $7.66\times10^{-2}$ | 0.686 | $1.35\times10^{5}$ |
| $X=0.5$ | $2.25\times10^{-2}$ | $4.32\times10^{-2}$ | $7.80\times10^{-2}$ | 0.638 | $7.59\times10^{4}$ |

duction of $Bi_2O_3$ into gadolinium-doped ceria can cause a small shift in the ceria peaks. This shift is indicative of change in lattice parameter. A distribution of different $Bi_2O_3$ concentrations within individual particles as well as between particles would lead to distribution of $2\theta$ values. Fig. 2 shows the lattice constant of $Ce_{0.8}(Gd_{1-x}Bi_x)_{0.2}O_{1.9}$ ceramics as a function of dopant concentration, $x$. Calculation of the cell parameters was carried out using the four main reflections typical of a fluorite structure material with a fcc cell, corresponding to the (1 1 1), (2 0 0), (2 2 0) and (3 1 1) plane. The lattice constant increased with increasing gadolinium amount. It indicates different radii of $Ce^{4+}$ (0.96 Å) and $Gd^{3+}$ (0.97 Å) in an oxide solid solution with a fluorite-type structure. Doping $Bi_2O_3$ in $CeO_2$ lattice will induce uniform strain in the lattice as the material is elastically deformed. This effect causes the lattice plane spacing to change and the diffraction peaks to shift to new $2\theta$ position. As the Bi content increasing, the lattice constant decreased linearly as a $(x) = 5.41204 - 0.0306x$ for $Ce_{0.8}(Gd_{1-x}Bi_x)_{0.2}O_{1.9}$ ceramics. It shows that these solid solution obey Vegard's rule.

The Arrhenius plot for the electrical conductivity of $Ce_{0.8}(Gd_{1-x}Bi_x)_{0.2}O_{1.9}$ ceramics is plotted in Fig. 3. The electrical conductivity is the bulk value, which is the sum of the grain interior, and grain boundary contributions.[7] Pure ceria is a poor ion conductor ($\sigma_{800\,^\circ C} \sim 2.41\times10^{-4}$ S/cm). The electrical conductivity is significantly enhanced in gadolinium-doped ceria ceramic by increasing oxygen vacancies ($V_o^{\bullet\bullet}$). The electrical conductivity of $Ce_{0.8}(Gd_{1-x}Bi_x)_{0.2}O_{1.9}$ increases systematically with increasing bismuth substitution and reaches a maximum for the composition of $Ce_{0.8}(Gd_{0.5}Bi_{0.5})_{0.2}O_{1.9}$ ($\sigma_{800\,^\circ C} \sim 7.80\times10^{-2}$ S/cm). With temperature increasing, the oxide ion mobility increases, and consequently the conductivities increase at high temperatures. Activation energy for conduction is obtained by plotting the electrical conductivity data in the Arrhenius relation for thermally activated conduction. Fig. 4 depicts the electrical conductivity of $Ce_{0.8}(Gd_{1-x}Bi_x)_{0.2}O_{1.9}$ as a function of temperature. With temperature increasing, the oxide ion mobility increases, and consequently the conductivities increase. Fig. 5 shows the variation of $E_a$ as a function of Bi substitution concentration in gadolinium-doped ceria ceramics in the temperature range of 500–850 °C. The activation energy decreases gradually with increasing Bi substitution concentration and reaches a value of $E_a = 0.638$ eV, for the $Ce_{0.8}(Gd_{0.5}Bi_{0.5})_{0.2}O_{1.9}$ specimen. Meanwhile, the pre-exponential factor also decreases with increasing Bi substitution concentration and reaches a minimum, $\sigma_o = 7.59\times10^4$ °C/cm, for the $Ce_{0.8}(Gd_{0.5}Bi_{0.5})_{0.2}O_{1.9}$ specimen. A summary of electrical conductivities, activation energies, and pre-exponential factor of $Ce_{0.8}(Gd_{1-x}Bi_x)_{0.2}O_{1.9}$ ceramics are listed in Table 2.

Apart from high ion conductivity, the electrolyte materials for SOFC must have matched thermal expansion coefficient for cathode and anode materials to avoid microcrack between anode and electrolyte or between cathode and electrolyte at operation temperature. Consequently, thermal expansion is an important property, it governed the performance of

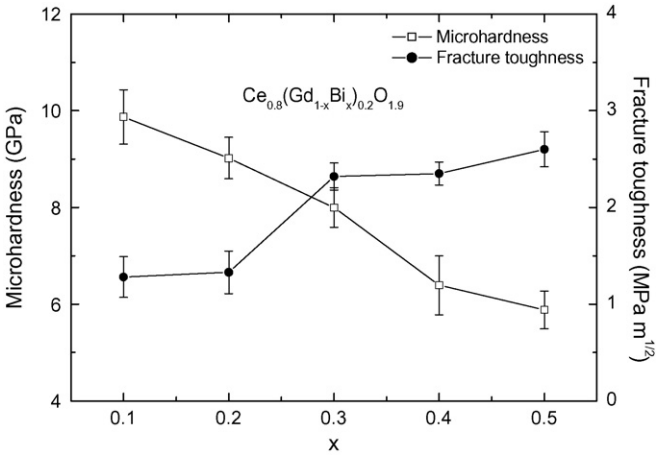


Fig. 8. Microhardness and fracture toughness, respectively, dependent of Bi amount for $Ce_{0.8}(Gd_{1-x}Bi_x)_{0.2}O_{1.9}$ ceramic.

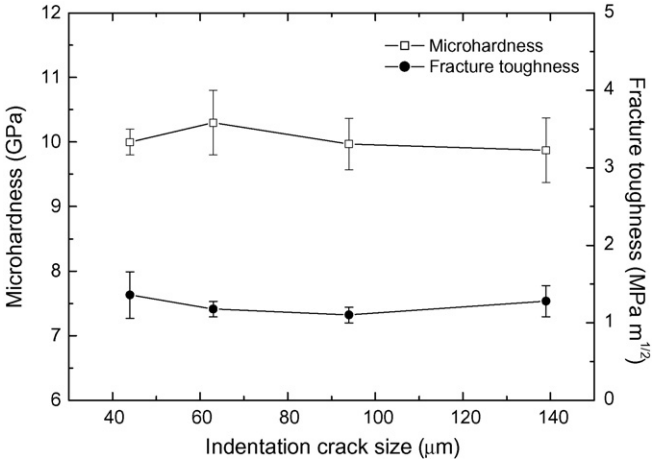


Fig. 9. Microhardness and fracture toughness, respectively, vs. indentation crack size for $Ce_{0.8}(Gd_{0.9}Bi_{0.1})_{0.2}O_{1.9}$ ceramic.

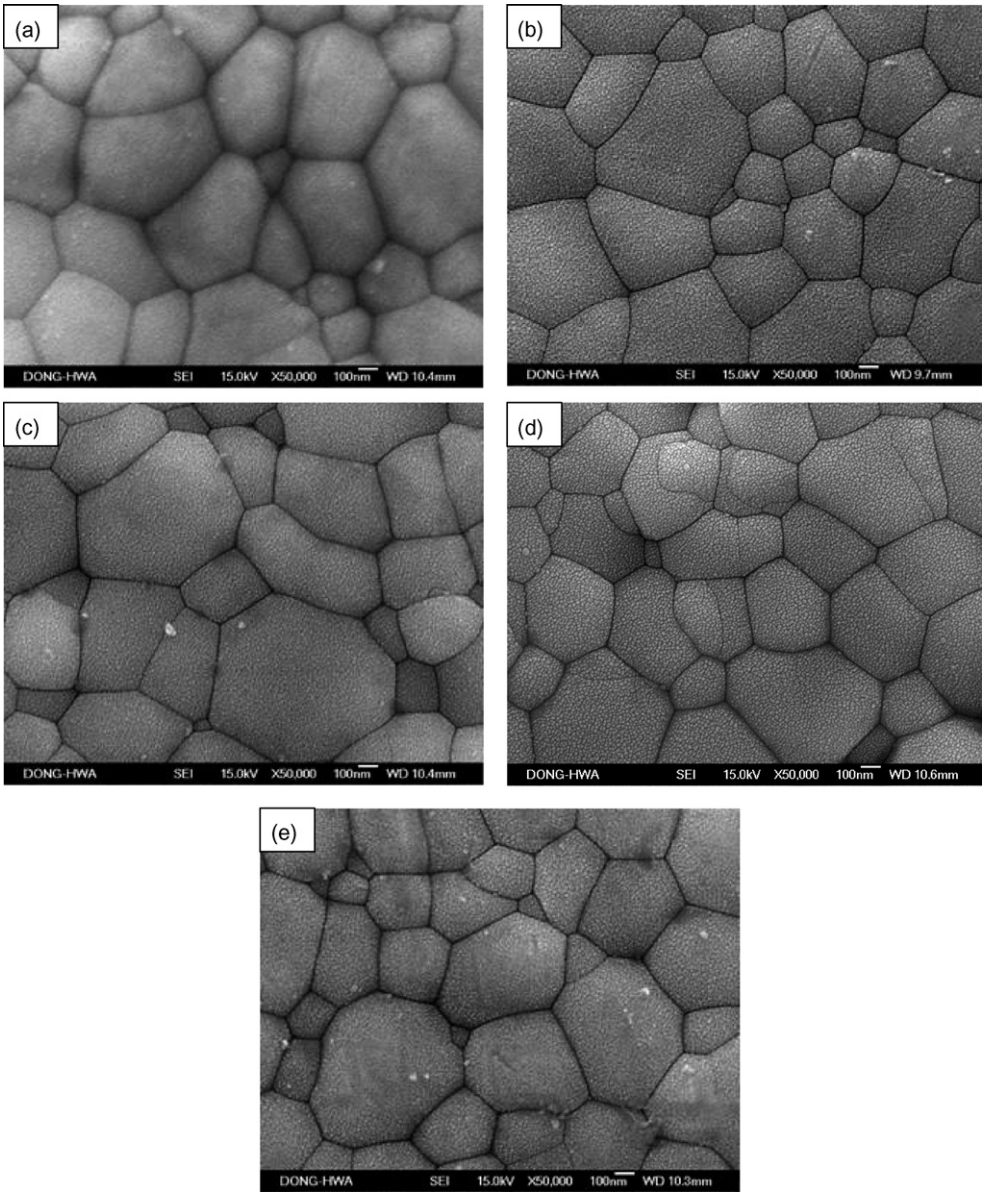


Fig. 10. Scanning electron micrograph of (a) $Ce_{0.8}(Gd_{-0.9}Bi_{0.1})_{0.2}O_{1.9}$ sintered at 1450 °C for 6 h, (b) $Ce_{0.8}(Gd_{-0.8}Bi_{0.2})_{0.2}O_{1.9}$, (c) $Ce_{0.8}(Gd_{-0.7}Bi_{0.3})_{0.2}O_{1.9}$, (d) $Ce_{0.8}(Gd_{-0.6}Bi_{0.4})_{0.2}O_{1.9}$ sintered at 1400 °C for 6 h and (e) $Ce_{0.8}(Gd_{-0.5}Bi_{0.5})_{0.2}O_{1.9}$ sintered at 1350 °C for 6 h.

high temperature devices. A bulk thermal expansion study on $Ce_{0.8}(Gd_{0.5}Bi_{0.5})_{0.2}O_{1.9}$ ceramics has been conducted from room temperature to 850 °C using a dilatometer. A typical plot of linear thermal expansion (in percent) as function of temperature is shown in Fig. 6. It revealed that linear thermal expansion fitted as a function of temperature using a polynomial regression. The polynomial correlations are given as follows (temperature, $T$, in Centigrade):

for $Ce_{0.8}(Gd_{0.9}Bi_{0.1})_{0.2}O_{1.9}$: 100

$$\Delta L/L_o = -0.04415 + (8.38904 \times 10^{-4})T + (1.2853 \times 10^{-6})T^2 - (5.67107 \times 10^{-12})T^3 + (2.79666 \times 10^{-13})T^4$$

for $Ce_{0.8}(Gd_{0.8}Bi_{0.2})_{0.2}O_{1.9}$: 100

$$\Delta L/L_o = -0.0456 + (8.95066 \times 10^{-4})T + (2.27352 \times 10^{-6})T^2 - (1.82719 \times 10^{-9})T^3 + (8.43327 \times 10^{-13})T^4$$

for $Ce_{0.8}(Gd_{0.7}Bi_{0.3})_{0.2}O_{1.9}$: 100

$$\Delta L/L_o = -0.05019 + (9.55119 \times 10^{-4})T + (1.82449 \times 10^{-6})T^2 - (5.7593 \times 10^{-10})T^3 + (1.16339 \times 10^{-13})T^4$$

for $Ce_{0.8}(Gd_{0.6}Bi_{0.4})_{0.2}O_{1.9}$: 100

$$\Delta L/L_o = -4.45765 \times 10^{-4} + (8.95081 \times 10^{-6})T + (2.0643 \times 10^{-8})T^2 - (1.37552 \times 10^{-11})T^3 + (6.20947 \times 10^{-15})T^4$$

for $Ce_{0.8}(Gd_{0.5}Bi_{0.5})_{0.2}O_{1.9}$: 100

$$\Delta L/L_o = -0.04442 + (7.08809 \times 10^{-4})T + (3.33656 \times 10^{-6})T^2 - (3.93743 \times 10^{-9})T^3 + (2.16177 \times 10^{-12})T^4.$$

The average thermal expansion coefficient (TEC) from 25 to 850 °C is presented in Fig. 7. The thermal expansion coefficient of $Ce_{0.8}(Gd_{1-x}Bi_x)_{0.2}O_{1.9}$ ($0.1 < x < 0.5$) is distribution in the range of 20.132–20.478 ppm/°C.

Fig. 8 depicted the fracture toughness and microhardness, respectively, versus Bi substitution for $Ce_{0.8}(Gd_{1-x}Bi_x)_{0.2}O_{1.9}$ ceramics. The fracture toughness versus crack size was first examined based on the equation as follows[8]:

$$K_{IC} = 0.016\left(\frac{E}{H_V}\right)^{1/2}\left(\frac{P}{C^{3/2}}\right)$$

where $K_{IC}$ is fracture toughness, $E$ is Young's modulus, $H_V$ is Vickers hardness, $P$ is the load and $C$ is the half crack size. There are many indentation equations for the calculation of $K_{IC}$ as presented by Poton and Rawling.[9] There are specific conditions and limitation for using there formulate; so far no universal formula is available to evaluate of $K_{IC}$ for all ceramics materials.[10] For convenience, above-mentioned equation is applied for dealing with the indentation data of doped ceria-based ceramics. The result revealed that the fracture toughness increased with Bi content. On the contrary, the microhardness decreased with Bi content for $Ce_{0.8}(Gd_{1-x}Bi_x)_{0.2}O_{1.9}$ ceramics. To realize the correlation between the indentation crack length and toughness, we used various load on indentation testing. Fig. 9 plots the relation between microhardness, fracture toughness and indentation crack length for $Ce_{0.8}(Gd_{0.9}Bi_{0.1})_{0.2}O_{1.9}$ ceramic. It is found that the indentation fracture toughness and microhardness are independent of crack length. Microstructure of $Ce_{0.8}(Gd_{1-x}Bi_x)_{0.2}O_{1.9}$ ceramics sintered in the range of 1350–1450 °C for 6 h are shown in Fig. 10. They showed good densification, well-sintered, no intragranular pores with a grain size ranging from 0.1 to 1 μm independent of Bi content. However, the addition of Bi can effectively decrease grain size, reduced sintering temperature and improve fracture toughness for gadolinium-doped ceria ceramics.

## 4. Conclusions

Recently, gadolinium-doped ceria powders have been studied widely due to it is a very important material of solid oxide fuel cells. In order to decrease sintering temperature, we attempt to add bismuth in gadolinium-doped ceria in current research. $Ce_{0.8}(Gd_{1-x}Bi_x)_{0.2}O_{1.9}$ ceramics sintering at 1350–1450 °C for 6 h, the maximum electrical conductivity,$\sigma_{800\,^\circ C} = 0.078$ S/cm with minimum activation energy, $E_a = 0.638$ eV was found at $Ce_{0.8}(Gd_{0.5}Bi_{0.5})_{0.2}O_{1.90}$ ceramic. The $Ce_{0.8}(Gd_{1-x}Bi_x)_{0.2}O_{1.9}$ powders synthesized by coprecipitation process can effectively decrease the sintering temperature, compared to that above 1550 °C required for gadolinium-doped ceria solid electrolytes prepared by solid state reaction.

The grain size in the range of 0.1–1 μm is independent of Bi content. The fracture toughness of $Ce_{0.8}(Gd_{1-x}Bi_x)_{0.2}O_{1.9}$ ceramic increased with Bi amount. It indicated that the mechanical stability of gadolinium-doped ceria ceramics could effectively improve by addition of bismuth. The oxide ion conductivity of $Ce_{0.8}(Gd_{1-x}Bi_x)_{0.2}O_{1.9}$ is higher than the most commonly used solid electrolyte, yttrium-stabilized zirconia. These ceramics with high conductivity are suitable for solid oxide fuel cells applications.

## Acknowledgement

The authors would like to thank the National Science Council of the Republic of China for financially supporting this research under contract no. NSC 95-2221-E-259-023.

## References

1. Su, X. T., Yan, Q. Z., Ma, X. H., Zhang, W. F. and Ge, C. C., Effect of co-dopant addition on the properties of yttrium and neodymium doped barium cerate electrolyte. *Solid State Ionics*, 2006, **177**, 1041–1045.
2. Minh, N. Q., Ceramic fuel cells. *J. Am. Ceram. Soc.*, 1993, **76**, 563–588.
3. Tuller, H. L. and Nowick, A. S., Defect structure and electrical properties of nonstoichiometric $CeO_2$ single crystals. *J. Electrochem. Soc.*, 1979, **126**, 209–217.
4. Hung, W., Shuk, P. and Greenblatt, M., Properties of sol-gel prepared $Ce_{1-x}Sm_xO_{2-x/2}$ solid electrolytes. *Solid State Ionics*, 1997, **100**, 23–27.
5. Chang, E. K. and Blumenthal, R. N., The nonstoichiometric defect structure and transport properties of $CeO_{2-x}$ in the near-stoichiometric composition range. *J. Solid State Chem.*, 1988, **72**, 330–337.
6. Chen, M., Hallstedt, B., Grundy, A. N. and Gauckler, L. J., $CeO_2$–CoO phase diagram. *J. Am. Ceram. Soc.*, 2003, **86**, 1567–1570.
7. Zha, S., Xia, C. and Meng, G., Effect of Gd(Sm) doping on properties of ceria electrolyte for solid oxide fuel cells. *J. Power Sources*, 2003, **115**, 44–48.
8. Anstis, G. R., Chantikul, P., Lawn, B. R. and Marshall, D. B., A critical evaluation of indentation techniques for measuring fracture toughness: I, direct crack measurements. *J. Am. Ceram. Soc.*, 1981, **64**, 533–538.
9. Poton, B. C. and Rawling, R. D., Vickers indentation fracture toughness test, Part 1. Review of literature and formulation of standard indentation toughness equations. *Mater. Sci. Technol.*, 1989, **5**, 865–872.
10. Ma, J., Zhang, T. S., Kong, L. B., Hing, P., Leng, Y. J. and Chan, S. H., Preparation and characterization of dense $Ce_{0.8}Y_{0.15}O_{2-\delta}$ ceramics. *J. Eur. Ceram. Soc.*, 2004, **24**, 2641–2648.